Revista Ciencia e Ingeniería Neogranadina
2025 enero - junio
Vol. 35(1) ISSN: 0124-8170 · e-ISSN: 1909-7735 ■ pp. 11-24
Editorial Neogranadina

DOI: https://doi.org/10.18359/rcin.7311

Characterization and Processing of Phosphate Rock as a Raw Material for Potential Use as Biomaterials

Gloria Soto Calle[a] ■ Néstor Rojas Reyes[b] ■ Adrián Gómez Zapata[c] ■ Sandra Díaz Bello[d]

Abstract: Seventy-five percent of the phosphate rock extracted is used for the production of phosphoric acid. However, during the leaching process, it is also possible to dissolve calcium compounds, allowing for the extraction of phosphorus and calcium ions from the resulting solution. This study focused on the application of hydrometallurgical processes directly to phosphate rock to obtain calcium phosphates with potential applications in the manufacture of biomaterials. After a physicochemical characterization of four phosphate rock samples, one sample was subjected to a hydrometallurgical process using nitric acid. The leachate was then neutralized with sodium hydroxide to achieve a pH between 4.5 and 12. One sample of the precipitate was dried at ambient temperature, while another was dried at 70°C. Depending on the pH and the Ca/P molar ratio, three types of calcium phosphates were obtained. X-ray diffraction analysis identified the three phases as octacalcium phosphate, hydroxyapatite, and monetite, all of which are recognized as biomaterials.

Keywords: Phosphate Rock; Mineral Characterization; Hydrometallurgical Processing; Product Diversification; Biomaterials

* Research Article

a Mining and Metallurgical Engineer, Mineral Institute – CIMEX, Medellín, Universidad Nacional de Colombia, Medellín, Colombia.
Email: gmsotoc@unal.edu.co; ORCID: https://orcid.org/0009-0007-4175-2208

b Ph. D. in Engineering, Master's in Engineering, Metallurgical Engineer, Mineral Institute – CIMEX, Medellín, Colombia. Universidad Nacional de Colombia, Medellín, Colombia.
Email: nrrojasr@unal.edu.co; ORCID: https://orcid.org/0000-0002-1644-471X

c Ph. D. in Engineering, Master's in Engineering, Instrumentation and Control Engineer, Institución Universitaria Pascual Bravo, Medellín, Colombia.
Email: adrian.gomez@pascualbravo.edu.co; ORCID: https://orcid.org/0000-0002-3536-1629

d Ph. D. in Engineering, Master's in Engineering, Metallurgical Engineer, Environmental and Natural Sciences Research Group – GICAN, Tunja, Colombia. Universidad Santo Tomás, Tunja, Boyacá.
Email: sandra.diazb@usantoto.edu.co; ORCID: https://orcid.org/0000-0002-8114-6655

Recibido: 6//05/2024 **Aceptado:** 29/10/2024 **Disponible en línea:** 11/04/2025

Cómo citar: Soto Calle, G., Rojas Reyes, N. R., Gómez Zapata, A., and Díaz Bello, S. (2025). Characterization and processing of phosphate rock as a raw material for potential use as biomaterials. *Ciencia E Ingeniería Neogranadina, 35*(1), 11–24. https://doi.org/10.18359/rcin.7311

Caracterización y procesamiento de roca fosfatada como materia prima para uso potencial como biomateriales

Resumen: El 75% de la roca fosfórica extraída se destina a la producción de ácido fosfórico, pero en el proceso de lixiviación también es posible disolver compuestos de calcio, permitiendo obtener iones de fósforo y calcio en la solución resultante. El presente trabajo se centró en la aplicación de procesos hidrometalúrgicos directamente a la roca fosfórica para la obtención de fosfatos de calcio con potencial aplicación para fabricación de biomateriales. Luego de una caracterización fisicoquímica de 4 muestras de roca fosfórica, una muestra de roca fosfórica fue sometida a un proceso hidrometalúrgico con ácido nítrico. El lixiviado se neutralizó con hidróxido de sodio a pH entre 4.5 y 12. Una muestra del precipitado se secó a temperatura ambiente y la otra a 70°C. Con este proceso, dependiendo del pH y la relación molar Ca/P se obtuvo tres tipos de fosfatos de calcio. A través de la difracción de rayos X se identificaron que las tres fases eran fosfato octacálcico, hidroxiapatita y monetita, las cuales son reconocidas como biomateriales.

Palabras clave: roca fosfórica; caracterización mineral; procesamiento hidrometalúrgico; diversificación de productos; biomateriales

Caracterização e processamento de rocha fosfática como matéria-prima para uso potencial como biomateriais

Resumo: Cerca de 75% da rocha fosfática extraída é destinada à produção de ácido fosfórico, mas, no processo de lixiviação, também é possível dissolver compostos de cálcio, permitindo a obtenção de íons de fósforo e cálcio na solução resultante. Este trabalho concentrou-se na aplicação de processos hidrometalúrgicos diretamente à rocha fosfática para a obtenção de fosfatos de cálcio com potencial aplicação na fabricação de biomateriais. Após uma caracterização físico-química de quatro amostras de rocha fosfática, uma delas foi submetida a um processo hidrometalúrgico com ácido nítrico. O lixiviado foi neutralizado com hidróxido de sódio, ajustando-se o pH entre 4,5 e 12. Uma amostra do precipitado foi seca à temperatura ambiente e outra a 70 °C. Com esse processo, dependendo do pH e da relação molar Ca/P, foram obtidos três tipos de fosfatos de cálcio. Por meio de difração de raios X, identificou-se que as três fases correspondem a fosfato octacálcico, hidroxiapatita e monetita, reconhecidos como biomateriais.

Palavras-chave: rocha fosfática; caracterização mineral; processamento hidrometalúrgico; diversificação de produtos; biomateriais

Introduction

Due to the similarity of their chemical composition to that of bones, teeth, and tissue, calcium phosphates (CaPs) are well-positioned as significant biomaterials for use in treatments such as tissue engineering, bone regeneration, dental implants, and controlled release systems [1,2]. Their ability to stimulate and promote cell growth has led to considerable research focused on improving the properties of these compounds [3,4].

According to the literature, most experimental studies on the synthesis of CaPs use pure reagents as starting materials. Tamimi et al. (2012) [4] and Shang et al. (2014) [5] indicate that different CaPs can be synthesized from solutions containing calcium (Ca^{2+}) and phosphate (PO_4^{3-}) ions.

Phosphorus (P) is typically found in association with other elements, including calcium (Ca), sodium (Na), fluorine (F), aluminum (Al), and magnesium (Mg). It is present in most rocks, particularly phosphate rocks, where phosphorus pentoxide (P_2O_5) may constitute 18 to 40% of the total volume, typically in the form of fluorapatite carbonate ($Ca_5(PO_4CO_3)_3F$) [6].

Acidulation of phosphate rock is a hydrometallurgical process used to produce phosphoric acid [7,8], a key component in fertilizer production (Li et al., 2020; Ma et al., 2018). In Colombia, 75% of the phosphate rock extracted is used for phosphoric acid production [9], a process that involves various acids, such as sulfuric, nitric, and hydrochloric acid, to obtain phosphorus-rich solutions [7,8]. However, due to the nature of phosphate rock, the leaching process can also dissolve impurities, including calcium compounds, thereby making both phosphorus and calcium ions available in the resulting solution [10].

By 2022, Colombia projected an annual phosphate rock production of approximately 41.5 kTn. That same year, the Colombian Geological Service identified four areas with high mineral potential for phosphate extraction, three of which are located in the department of Boyacá [11].

Phosphate rock has been extensively used to produce various types of fertilizers [12-16]. It has also been studied for the extraction of trace elements such as rare earths and uranium [17-21]. However, there is limited literature on the direct extraction of biomaterials from phosphate rock [22,23], particularly using processes like the sol-gel method [23] or employing calcium nitrate ($Ca(NO_3)_2$) or calcium chloride ($CaCl_2$) as precipitators, or processes involving high pressures and temperatures [24].

The objective of this study is to physicochemically characterize four phosphate rock samples and explore the application of hydrometallurgical processes to obtain calcium phosphates, with potential applications in the field of biomaterials.

Materials and Methods

Mineral samples

The mineral is extracted using the rock fragmentation method with explosives. From the material collected in this process from each mining fronts, samples were randomly selected for this study. The mining company was responsible for the sample collection. Four mineral samples, labeled M1 to M4 for the project, were processed from different mines located in the department of Boyacá, Colombia. Approximately 50 kg of each sample was subjected to a particle size reduction process using jaw and roller crushers, followed by sieving to obtain representative quantities of each sample with particle sizes smaller than 74 μm. The chemical composition, mineralogical species, and thermal behavior of these samples were determined using techniques such as X-ray fluorescence (XRF), X-ray diffraction (XRD), Thermogravimetric analysis (TGA), and Differential Scanning Calorimetry (DSC). The samples then underwent an acidulation process using sulfuric, nitric, and phosphoric acids at varying concentrations and durations to explore potential routes for obtaining higher-value by-products.

Compositional Analysis

This analysis was conducted using an Epsilon Range 13V 1.5 Malvern Panalytical X-Ray Fluorescence (XRF) System and an Oxford Instruments EDS probe coupled to a JEOL JSM-5910LV Scanning Electron Microscope (SEM). Conventional software and protocols were used and adapted to obtain the

required measurements. The characterization was performed on the powdered materials that made up the raw material samples M1 – M4. Using the different techniques and software, the elemental chemical composition was identified and quantified in terms of its oxide configuration, and the data were recorded in tables.

Mineralogical analysis

The spectra for the analyses were obtained using an Empyrean Panalytical XRD system, with operating conditions set for a sweep in the 2θ axis from 5° to 70°, with steps of 0.02° and a period of 0.5 s per step. Cu radiation with a wavelength (λ) of 1.5406 Å was used. Phase identification and analysis were performed using X'Pert HighScore Plus software. The characterization was carried out for all raw material samples and at different stages during their processing. Diffractograms were obtained, and the analysis allowed for the determination of the number of phases present, the lattice parameters of these phases, and the volume of the unit cell representing each phase, semiquantitatively.

To complement the structural analysis of the samples, the vibrational modes of the compounds in the rocks were determined through Raman spectroscopy, using Thermo Scientific equipment (reference 912A0999) and laser sources with wavelengths of 532 and 636 nm.

Thermal analysis

Tests to determine the thermal behavior as a function of time and mass loss with temperature were performed using a TRIOS SDT650 TA Instruments thermogravimetric analyzer equipment. Each sample was subjected to a heating ramp of $10°C \cdot min^{-1}$, with a sweep from room temperature to 1140°C, using approximately 50 mg of powdered samples placed in alumina crucibles in an inert nitrogen (N_2) atmosphere. During the tests, data for the reconstruction of the Thermogravimetric (TG) curve and the Derivative Thermogravimetric analysis (DTG) were recorded using the equipment's software. From the analysis of the curves, it was possible to identify the main temperature points at which mass loss events occurred due to endothermic or exothermic processes, as well as phase transformations of the sample components.

Design of experiments

The experiments were conducted on the sample with the lowest phosphorus content to observe its behavior and response to the hydrometallurgical process. For this purpose, several tests were performed at different concentrations of nitric acid (ranging from 2M to 5M) and varying pH levels (ranging from 4 to 12), in order to evaluate the species that could be obtained under these two variables. This type of experimental design is called a simple comparative experiment [25, 26], which allows for the analysis of the behavior of a representative sample with two variables (pH and HNO_3 concentration), with a response variable, such as the precipitate or product generated under these specific conditions.

Hydrometallurgical Processing

Sample M1 was subjected to a particle size reduction and classification process, including crushing, grinding, and sieving, until it reached a size where 80% of the particles were smaller than 103 µm. A 75 g portion of the sample was mixed with 3 M HNO_3 in a 1:3 ratio, and the resulting solution was mechanically agitated for 24 hours. After this period, the solid phase was separated from the liquid phase by filtration. To 25 mL of the obtained liquor, rich in P and Ca ions, constant volumes of 0.1 M NaOH were added while maintaining magnetic agitation until pH values between 4.5 and 12 were achieved. These experimental parameters were determined based on the work of Soto-Calle et al. [27]. Once the desired pH values were reached, the agitation was stopped, allowing the differentiation of two phases: one completely aqueous and colorless, and the other a white solid phase. The white solid phase, separated by filtration, was washed several times to remove contaminating ions such as nitrates, chlorides, and others. This solid phase was then divided into two equal parts. One part was dried at room temperature in a covered beaker for 3 weeks and was labeled as CaP1. The other part was dried in an oven at 70°C on a heating plate for

60 minutes and was labeled as CaP2. This entire process was repeated three times. Both CaP1 and CaP2 samples were subjected to compositional and structural characterization.

Results and Discussion

Compositional and Mineralogical Analysis of the Pr

XRF

The results obtained by XRF for the elemental composition of samples M1 – M4 are presented in Table 1. Table 1 shows that the main compositional differences between the samples are related to the amounts of P, Ca, Si, Mg, and S, while Ti, Mn, Fe, and Sr are present in smaller quantities. Based on the content ranges of P and alkaline earth metals such as Ca and Mg, as well as other elements like Si, the phosphate rock samples were categorized as medium-grade colophonite minerals [28]. The X-ray fluorescence (XRF) software provides a quantitative analysis based on the formation of oxides from their metals. According to Nazarbekova et al. [29] and Toama et al. [30], the ratio of CaO to P_2O_5 contents should be less than 1.6 to ensure efficient sulfuric acid consumption in the production of phosphoric acid. In the results obtained (see Table 1), the ratios for samples M1 – M4 were 1.38, 1.30, 1.45, and 1.63, respectively. As seen, sample M4 had a ratio above the recommended value, making it a focus of research interest for potential diversification of phosphate rock production from this mining front.

Table 1. Elemental chemical composition analysis and stoichiometric oxides in phosphate rock samples

Sample	Element [%]											
	P	Ca	Si	Mg	S	Cl	K	Al	Ti	Mn	Fe	Sr
M1	13.44	36.76	12.48	3.54	0.08	0.33	0.23	1.29	0.09	0.02	1.06	0.15
M2	15.09	39.15	11.04	3.76	0.04	0.26	0.15	1.17	0.07	0.02	0.78	0.14
M3	15.22	44.20	6.81	4.03	0.07	0.26	0.08	1.05	0.06	0.07	0.91	0.23
M4	13.27	43.36	5.26	5.57	0.26	0.21	0.06	0.90	0.06	0.02	0.68	0.28
Sample	**Oxide [%]**											
	P_2O_5	CaO	SiO_2	MgO	SO_3	K_2O	Al_2O_3	TiO_2	MnO	Fe_2O_3	SrO	
M1	26.81	37.00	7.00	6.89	0.15	0.21	2.45	0.09	0.02	0.92	0.10	
M2	29.53	38.39	22.13	6.43	0.08	0.14	2.16	0.06	0.01	0.66	0.09	
M3	30.98	44.77	13.86	6.89	0.13	0.07	1.96	0.06	0.05	0.80	0.16	
M4	28.61	46.61	11.25	10.01	0.56	0.06	1.74	0.06	0.02	0.64	0.21	

Source: The authors.

It is recommended that, in terms of P_2O_5 content, the ratio of the sum of the mineral content of Al_2O_3 + Fe_2O_3 should be between 0.08 and 0.1 [31] to facilitate the production of phosphoric acid. In this regard, values of 0.13, 0.10, 0.09, and 0.08 were found for samples M1 – M4, respectively, with the least favorable value for producing this acid being found in sample M1. Additionally, it should be noted that the presence of Al_2O_3 is undesirable, as it may lead to the formation of insoluble phosphates, which decrease the content of water-soluble P_2O_5.

Regarding the K content in the samples, it is important to note that only in M1, where the values were highest, might the levels be high enough to cause sedimentation (sludge) in machinery. The subsequent removal of this sludge would not be routine or easy, as the element reacts with fluorine and silica to form fluorosilicates (K_2SiF_6), which are difficult to eliminate from the process.

Finally, it is worth mentioning that if the F content in the samples could be accurately quantified, the fluorine complexation ratio (FCR), defined

by the following expression, can be determined using Equation 1:

$$FCR = \frac{0.0536 * \%F}{(0.0588 * \%Al_2O_3) + (0.0667 * \%SiO_2)} \quad (1)$$

Equation 1 defines the filterability of phosphoric sludge. To prevent major issues in the process, the FCR value should be between 0.42 and 1.378. Values below the lower limit significantly reduce filterability due to the presence of undissolved silica salts and poor crystallization. In conclusion, the FCR parameter should be considered when studying reaction kinetics [32]. By considering the limit values for the FCR, it may be possible to establish acceptable limits for the F content in the samples. These ranges would be 31.04–33.47, 27.57–29.76, 17.36–19.33, and 13.47–15.13 for samples M1 – M4, respectively.

XRD

Table 2 presents the main mineralogical phases of samples M1 – M4, as determined from the XRD spectra and the semi-quantitative analysis conducted using the software.

Figure 1A displays the diffraction spectra for the analyzed samples, which are overlaid due to the low variability in the quantities of the quantified phases, as confirmed by the data in Table 2. The insets on the right side of Figure 1A show an enlargement of the peaks, corresponding to an intensity of 100% for each identified phase. The positions and planes on the 2θ axis, based on the identified pattern chart, are as follows: 31.94(4)° (2 1 1) for Fluorapatite (FA), 26.64(6)° (0 1 1) for Quartz (Qz), and 29.45(2)° (1 0 4) for Calcite (CaC). The peak height (intensity) is related to the percentage of each phase, which aligns with the data presented in Table 2.

Table 2. Mineralogical Phases Present in the Phosphate Rock Samples with their Respective Lattice Parameters and Crystalline Cell Volumes

Sample	Mineralogical Phase [%]		
	Fluorapatite $Ca_5(PO_4)_3F$	Quartz SiO_2	Calcite $CaCO_3$
M1	59	34	7
M2	54	41	5
M3	67	27	6
M4	55	41	4
Mineralogical Phase	**Cell Parameters [Å]**			**Volume of Unit Cell [Å^3]**
	A	***b***	***C***	
Fluorapatite (Hexagonal)	9.363	9.363	6.878	522.18
Quartz (Hexagonal)	4.912	4.912	5.404	112.93
Calcite (Rhombohedral)	4.99	4.99	17.002	366.63

Source: The authors.

Figure 1. A X-ray diffraction spectra for the samples analyzed. B) Raman spectra for the phosphate rock samples

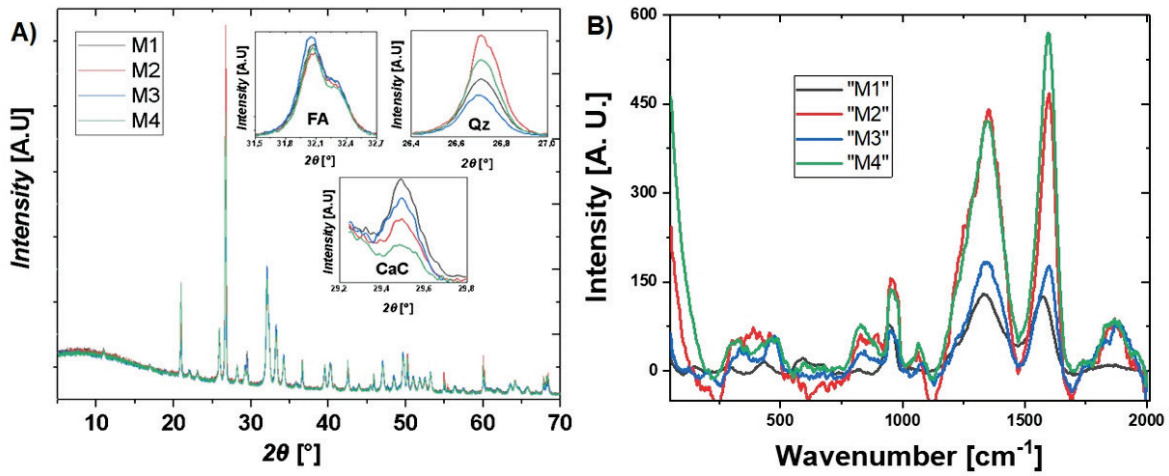

Source: The authors.

Table 2 presents the values for the lattice parameters and cell volumes of the various crystalline systems identified in the three main mineralogical phases detected across the different samples. Additionally, the phase patterns are indexed in the consulted database with the following codes: 01-071-0880 for Fluorapatite, 01-078-2315 for Quartz, and 01-072-1652 for Calcite.

Raman

Figure 1B presents the Raman spectra of the samples, highlighting the behavior of their different vibrational modes. Similarities are observed between samples M1 and M3, as well as between samples M2 and M4, with samples M2 and M4 showing peaks of greater intensity compared to the others.

Table 3. Wavenumber Values for the Different Vibrational Modes Detected in the Samples

Sample	Wave number [cm^{-1}]						
M1	1870	1576	1330	---	1022	944	433
M2	1869	1600	1351	1063	---	952	389
M3	1874	1600	1334	1076	---	952	477
M4	1855	1596	1342	1064	---	953	466
Vibration Mode	Magnesite	Carbonates	CO_3^{2-}, Yes	$\nu_3 PO_3^{2-}$	$\nu_1 CO_3^{2-}$	$\nu_1 PO_3^{2-}$	$\nu_2 PO_3^{2-}$

Source: The authors

Table 3 presents the wavenumber values (in cm^{-1}) for the various vibrational modes observed in the samples, as shown in Figure 1B. According to the references consulted, wavenumbers between 389 and 477 cm^{-1} can be attributed to the $\nu_2(PO_3^{2-})$ vibrational mode, those between 944 and 959 cm^{-1} to the $\nu_1(PO_3^{2-})$ vibrational mode, and 1022 cm^{-1} for sample M1 to the $\nu_1(CO_3^{2-})$ mode. Wavenumbers between 1063 and 1076 cm^{-1} correspond to the $\nu_3(PO_3^{2-})$ vibrational mode for samples M2 to M4. Wavenumbers between 1330 and 1351 cm^{-1} are likely associated with impurities of CO_3^{2-} and/or silicon. Similarly, values between 1576 and 1600 cm^{-1} may be linked to the presence of carbonates. Finally, wavenumbers between 1855 and 1874 cm^{-1} are attributed to the presence of magnesite [33-36].

Thermal analysis of phosphate rocks

The results obtained from TGA for samples M1 – M4 are shown in Figure 2. The temperature values at which peaks were generated, reflecting phase changes and mass loss in the different minerals that make up the phosphate rocks, can be observed. Figure 2A presents the mass loss curves, while Figure 2B shows the TGA derivative, where the peaks corresponding to phase changes for each sample can be identified.

Figure 2A reveals that sample M4 exhibits the greatest mass loss from room temperature to 1140°C, approximately 7.8%, followed by samples M3 (5.3%), M1 (3.9%), and M2 (3.5%). These findings align with previous studies [37,38], although those were conducted with air and CO_2 as the carrier gas. The mass loss as a function of temperature for different intervals is summarized in Table 4.

The first stage (room temperature to 200°C) corresponds to the evaporation of moisture and water in the sample. The interval between 200°C and 600°C is attributed to the crystallization of powders from the amorphous phase, as observed in Figure 1A (between 5° and 20° on the 2θ axis). Sample M1 showed the highest amount of amorphous phase, followed by M4, M3, and M2, with values of 1.7%, 1.4%, 1.0%, and 0.6%, respectively. This is likely due to the $CaCO_3$ content in M1, as seen in Figure 1A.

The final stage (600°C to 1140°C) corresponds to the main mass loss for each sample, with mass losses of 5.6%, 3.0%, 2.1%, and 1.9% for M4, M3, M1, and M2, respectively. This stage represents the largest mass loss, with percentages of 73%, 57%, 54%, and 55%, in the same order as above.

Figure 2B presents the derivative TG showing some exothermic peaks between 700°C and 900°C. For samples M1, M2, and M3, the peaks occurred at 854°C, 882°C, and 872°C, respectively, which may be associated with the calcite phase. Ideally, the peak for calcite purity should be around 915°C [39]. The displacement of the peak for sample M4 to 834°C, the lowest of the four, could be linked to the semi-quantitative analysis results for this phase, as found by XRD and reported in Table 2. Additionally, for all samples, Figure 2B shows peaks at around 1088°C, 1050°C, 1031°C, and 1080°C, respectively. These peaks, along with those at 44°C, 97°C, 94°C, 45°C, 98°C, and 58°C, are likely associated with the fluorapatite phase. The mass losses for the samples are consistent with those reported by Stanić et al. (2015) [40] for fluorapatite samples synthesized through neutralization methods at the nanometer scale, as also shown in Table 3.

Figure 2. A) TG curves for the phosphate rock samples. B) DTG curves for the phosphate rock samples

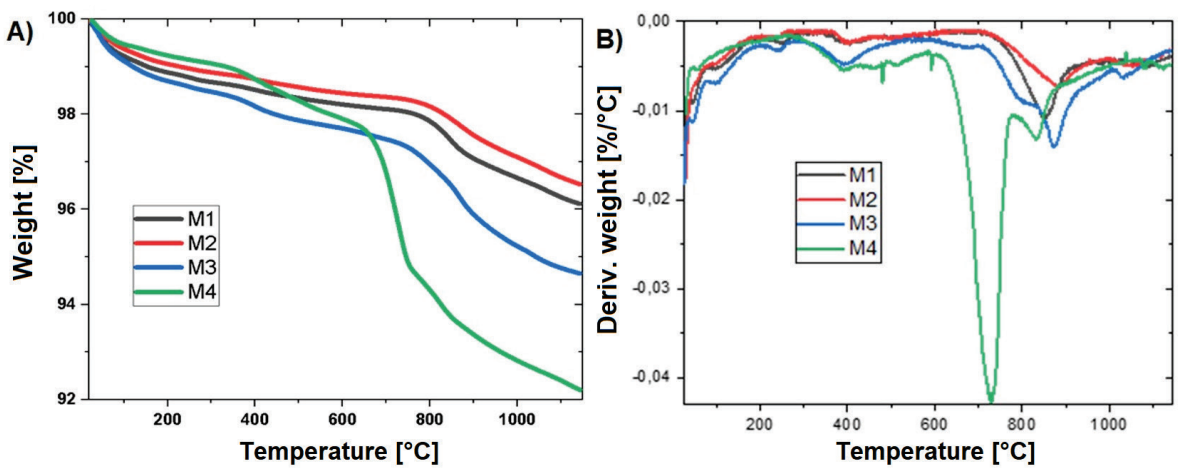

Source: The authors.

Table 4. Mass loss weight for samples as a function of temperature for different stages.

Temperature [° C]	Mass loss weight [%]			
	M1	M2	M3	M4
Room - 200	0.110	0.939	1.295	0.753
200 - 400	1.367	0.321	0.533	0.527
400 - 600	0.312	0,296	0.462	0.821
600 - 800	0.336	0.269	0.759	3.681
800 - 1140	1.735	1.624	2.280	1.965

Source: The authors

Calcium phosphate processing

Based on the results of the compositional, structural, and thermal characterization of the phosphate rock samples as raw materials for obtaining high-value by-products, sample M1 was selected. This decision was made because it had the lowest phosphorus and calcium content among all the samples, making it of particular research interest due to the reduced likelihood of obtaining calcium phosphates with high added value. It is hypothesized that if calcium phosphate by-products can be successfully extracted from this sample, there is a greater chance of obtaining them from samples with higher phosphorus and calcium contents. Another advantage of implementing a hydrometallurgical process for this sample is its lower organic matter content, as evidenced by the lower mass loss detected in the TGA tests. This results in a less complex leaching and filtration process, with a reduced risk of contamination.

The phosphorus and calcium-rich liquor obtained from the HNO3 leaching of sample M1 was neutralized with NaOH to pH values ranging from 4.5 to 12. During this process, a white solid phase precipitated. This solid phase was divided into two parts: one was air-dried and labeled as CaP1, while the other was oven-dried and labeled as CaP2.

Compositional analysis of calcium phosphates

The results obtained by XRF for the elemental composition of samples CaP1 and CaP2 are presented in Table 5. This table shows that the heat-treated sample, CaP2, had a 5.3% higher phosphorus (P) content than sample M1 (Table 1). This demonstrates the effectiveness of the hydrometallurgical process, which was further enhanced by the application of low-temperature thermal treatment to concentrate phosphorus from the phosphoric rocks. According to Garrido-Hernández et al. (2022) [3], a specific Ca/P molar ratio exists that not only facilitates the classification of calcium phosphates but also helps to understand and determine the biological functions they can fulfill. However, when calculating the molar ratios for the laboratory-produced samples, the results for CaP1 and The molar ratios for CaP1 and CaP2 were 2.71 and 1.75, respectively, indicating that the ratios reported in the literature do not correspond to a specific standard species. This opens the possibility for the formation of different species of calcium phosphate in the final process, thereby enhancing the potential for diversifying the by-products with added value that could be obtained from these raw materials.

Mineralogical analysis of calcium phosphates

Figure 3 shows the XRD spectrum of the referenced sample CaP1 (black) overlaid with that of sample CaP2 (red), highlighting the characteristic peaks of the principal mineralogical phases identified in each sample. These phases are reported in Table 5, which also presents the percentages found in the samples. Additionally, Table 5 includes the values for the lattice parameters and cell volumes of the different crystalline systems corresponding to the four main mineralogical phases detected.

The upper right inset of Figure 3 provides an enlargement of the peaks for the referenced sample CaP1 in the Octacalcium Phosphate (OCP) phase, identified with code 00-026-1056 at 31.55(5)° on the 2θ axis. The lower right inset shows an enlargement of the peaks for the Monetite (M) phase, identified with code 01-070-1425 at 30.24(1)°, and for the Hydroxyapatite (HAp) phase, with code 01-076-0694, exhibiting peaks at 31.77(1), 32.19(1), and 32.90(6)°, based on the mineralogical database used for identifying sample CaP2.

In the spectra of Figure 3, the triple peak characteristic of the HAp phase in sample CaP2 is clearly visible, along with the presence of the Monetite (M) phase. This confirms that the thermal treatment applied at a low temperature (70°C) to sample CaP2 was effective in transforming the material and optimizing the hydrometallurgical process for obtaining valuable by-products from phosphate rock. The increase in the quantity of the HAp phase, promoted by this thermal treatment, provided the necessary kinetic energy to accelerate the transformation of OCP into higher-purity phosphates, such as HAp and M, thereby enhancing the added value of the product.

Table 5. Elemental Composition Analysis, Mineralogical Phases Identified and Lattice Parameters and Crystalline Cell Volume in the Calcium Phosphate Samples Obtained From Phosphate Rock

Sample	Element [%]										
	P	Ca	Mg	Si	Al	Cl	K	Ti	Mn	Fe	Sr
CaP1	9.15	34.12	5.73	0.46	0.77	0.98	0.0	0.02	0.02	0.83	0.11
CaP2	14.15	32.9	8.71	0.38	0.69	0.35	0.01	0.02	0.01	1.73	0.10

Sample	Mineralogical Phase [%]		
	OCP $Ca_8H_{12}O_{29}P_6$	HAp $Ca_5(PO_4)_3(OH)$	M $CaHPO_4$
CaP1	88	12	---
CaP2	---	56	44

Mineralogical Phase	Cell Parameters [Å]			Volume of Unit Cell [Å3]
	a	*b*	*C*	
OCP (Triclinic)	9.529	18.994	6.855	1220.57
HAp (Monoclinic)	9.421	18.843	6.881	1057.96
M (Triclinic)	6.910	6.627	6.998	309.28

Source: The authors

Figure 3. X-ray diffraction spectra for value-added phosphate samples obtained from phosphate rock

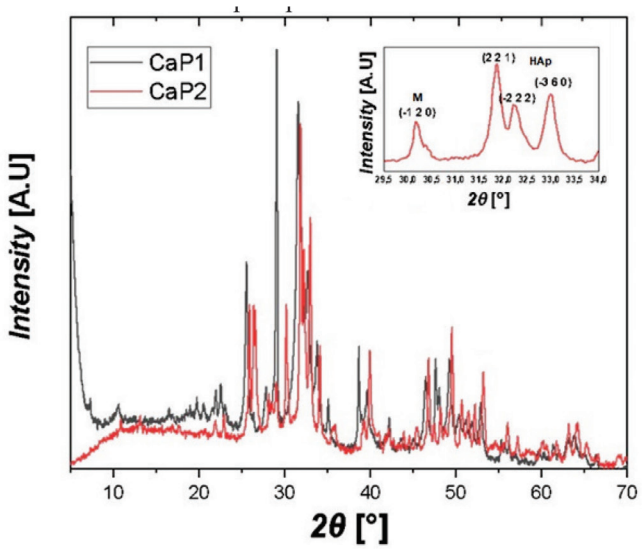

Source: The authors.

From the data presented above, it is evident that it is feasible to obtain three types of calcium phosphates by controlling the pH during the precipitation process: Octacalcium Phosphate (OCP), Hydroxyapatite (HAp), and Monetite (M) [41-44]. Calcium phosphates are widely utilized in biomedical applications due to several key characteristics: they are similar to the organic component of bone, making them ideal for bone repair; they exhibit osteoconductivity, forming an interface that promotes both chemical bonding and the guided formation of new bone tissue; and they are used as calcium phosphate cements, which typically consist of two components—cement powder and cement solution. The powders are often mixtures of different calcium phosphates. Additionally, the incorporation of macropores in calcium phosphate materials can facilitate bone ingrowth and accelerate the replacement of the cement with bone. Beyond calcium phosphate coatings, osteoconductive biomaterials can be combined with other biomaterials to create osteoconductive composites. For instance, calcium phosphate ceramics, bioglass or glass ceramics, when combined with polymers or collagen particles, retain osteoconductive properties [45-48].

Given that the species obtained in this study are derived from a natural resource, it is necessary to develop purification methods and complement them with biocompatibility studies to ensure their suitability for medical applications. It is important to note that while the synthesis of species such as hydroxyapatite, monetite, and enriched calcium phosphates is well-established through defined chemical routes, obtaining these species from phosphate rock for use in biomaterials is an innovative process. This process is particularly challenging due to the mineralogical composition of phosphate rock, which contains fluorine. Fluorine complicates the decomposition of the material, making the generation of these products more difficult. While conventional chemical treatments have been explored in the literature, this work demonstrates that phosphate rock offers the opportunity to obtain novel species that could have significant applications in bioengineering.

Conclusions

Mineralogically, phosphate rock is considered the primary source of phosphorus (P). Through characterization techniques, an elemental chemical and mineralogical analysis of phosphate rock from Boyacá, Colombia, was conducted. The findings revealed that the predominant species in the rock vary, with fluorapatite comprising between 54% and 67%, quartz between 27% and 41%, and calcite between 4% and 7%. The elemental chemical analysis showed phosphorus pentoxide (P_2O_5) content ranging from 26.8% to 30.9%, indicating that these deposits are promising candidates for the diversification of phosphate-based products.

Leaching phosphate rock with nitric acid generates solutions containing available phosphorus and calcium ions. By adjusting temperature and pH, the formation of calcium phosphates such as hydroxyapatite, monetite, and octacalcium phosphate is facilitated. Calcium phosphates are primarily used in biomedical applications. However, since these compounds are derived from a natural source, developing purification methods, accompanied by biocompatibility studies, is essential.

The objective of this study was to explore an alternative route for diversifying products using phosphate rock as raw material. Despite the growing interest, the available information on the synthesis of calcium phosphates from this source remains limited. This knowledge gap underscores the need for further research in this area, opening opportunities for the development of new processes and products based on the efficient processing of phosphate rock.

Aknowledgments

This work was funded by the Universidad Nacional de Colombia, Medellín, and the MinCiencias project SGR - CTI call 006-2019, BPIN 2020000100507, internal code 74957.

References

[1] A. Carlos and A. Herrera, "Fosfatos de cálcio de interesse biológico: importância como biomateriais, propriedades e métodos de obtenção de recobrimentos," *Química Nova,* vol. 36, no. 6, pp. 1352-1358, 2010. DOI: https://doi.org/10.1590/S0100-40422010000600025

[2] L. Medvecky, R. Stulajterova, M. Giretova, T. Sopcak and V. Girman, "Reinforcement of hydroxyapatite ceramics by soaking green samples of tetracalcium phosphate / monetite mixture in aqueous solutions," *Ceramics International*, vol. 48, no. 12, pp. 17776–17788, 2022. DOI: https://doi.org/10.1016/j.ceramint.2022.03.048

[3] A. Garrido-Hernández, G. García-Domínguez, J. Reyes-Miranda, M.A. Camacho-González, L. Chávez-Güitrón and J.M. Castillo-Minjárez, (2022). "Evaluación de la citotoxicidad de fosfatos de calcio sintetizados a diferentes relaciones molares de Ca/P por la vía hidrotermal," *Pädi Boletín Científico de Ciencias Básicas e Ingenierías Del ICBI*, vol. 10, (Especial7), pp. 183–188, 2022. DOI: https://doi.org/10.29057/icbi.v10iespecial7.9957A

[4] F. Tamimi, Z. Sheikh and J. Barralet, "Dicalcium phosphate cements: Brushite and monetite," *Acta Biomaterialia*, vol. 8, no. 2, pp. 474–487, 2012. DOI: https://doi.org/10.1016/j.actbio.2011.08.005

[5] H.B. Shang, F. Chen, J. Wu, C. Qi, B.Q. Lu, X. Chen and Y.J. Zhu, "Multifunctional biodegradable terbium-doped calcium phosphate nanoparticles: facile preparation, pH-sensitive drug release and in vitro bioimaging," *RSC Journals*, vol. 4, pp. 53122-53129, 2014.DOI: https://doi.org/10.1039/C4RA09902H

[6] L.N. Castro and R.J. Melgar, R. *Minerales para la Agricultura en Latinoamérica*. Capítulo III Fosfatos, Rocas Fosfóricas. Argentina, CYTED, 2005, pp. 37-82. http://fosfatos.gl.fcen.uba.ar/index.php/bibliografia-de-consulta/

[7] C. Avşar and A.O. Gezerman, "An evaluation of phosphogypsum (PG)-derived nanohydroxyapatite (HAP) synthesis methods and waste management as a phosphorus source in the agricultural industry," *Medziagotyra*, vol. 29, no. 2, pp. 247–254, 2023. DOI: https://doi.org/10.5755/j02.ms.31695

[8] I. Bouchkira, A.M. Latifi, L. Khamar and S. Benjelloun, "Modeling and multi-objective optimization of the digestion tank of an industrial process for manufacturing phosphoric acid by wet process," *Computers and Chemical Engineering*, vol. 156, 2022. DOI: https://doi.org/10.1016/j.compchemeng.2021.107536

[9] N.M. Espinel Pérez, "Synthesis of thermophosphate fertilizers by a plasma torch," *Organic Fertilizers - New Advances and Applications,* Mar. 28, 2023. DOI: 10.5772/intechopen.1001352

[10] U. Ryszko, P. Rusek and D. Kołodyńska, "Quality of phosphate rocks from various deposits used in wet phosphoric acid and P-fertilizer production," *Materials*, vol. 16, no. 2, 2023.DOI: https://doi.org/10.3390/ma16020793

[11] G. Martínez, N. Rojas, R. Terraza, C. Martín, and S. Rojas, "Geological mapping for phosphate in the central region of the Eastern Cordillera, Department of Boyacá, Colombia," *Boletín Geológico*, vol. 50, no. 1, 2023. DOI: https://doi.org/10.32685/0120-1425/bol.geol.50.1.2023.666

[12] J.C. Hughes and R.J. Gilkes, "The effect of chemical extractant on the estimation of rock phosphate fertilizer dissolution," *Australian Journal of Soil Research,* vol. 22, no. 4, pp. 475 – 481, 1984. DOI: https://doi.org/10.1071/SR9840475

[13] Z. Benredjem, R. Delimi, "Use of extracting agent for decadmiation of phosphate rock," *Physics Procedia*, vol. 2, no. 3, pp. 1455-1460, 2009. DOI: https://doi.org/10.1016/j.phpro.2009.11.116

[14] F. Habashi, "Solvent extraction in the phosphate fertilizer industry," *EPD Congress, The Minerals, Metals and Materials Society,* pp. 201-218, 1998. https://www.researchgate.net/profile/Fathi-Habashi/publication/233389507_Solvent_extn_phosphate_ind/links/09e4150a1192a3cce8000000/Solvent-extn-phosphate-ind.pdf

[15] P. K. Ghosal and T. Chakraborty, "Comparative solubility study of four phosphatic fertilizers in different solvents and the effect of soil," *Resources and Environment*, vol. 2, no. 4, pp. 175-179, 2012. DOI: 10.5923/j.re.20120204.07

[16] N.S. Bolan, and M.J. Hedley, "Dissolution of phosphate rocks in soils. 1. Evaluation of extraction methods for the measurement of phosphate rock dissolution,". *Fertilizer Research*, vol. 19, pp. 65–75, 1989. DOI: https://doi.org/10.1007/BF01054677

[17] S. Wu, L. Wang, L. Zhao, P. Zhang, H. El-Shall, B. Moudgil, X. Huang and L. Zhang, "Recovery of rare earth elements from phosphate rock by hydrometallurgical processes – A critical review," *Chemical Engineering Journal*, vol. 335, pp. 774-800, 2018. DOI: https://doi.org/10.1016/j.cej.2017.10.143.

[18] M. Chen and T.E. Graedel, "The potential for mining trace elements from phosphate rock," *Journal of Cleaner Production*, vol. 91, no. 337-346, 2015. DOI: https://doi.org/10.1016/j.jclepro.2014.12.042;

[19] N.A. Khaledi, M. Taha, A. Hussein, E. Hussein, A.E. Yahyaoui and N. Haneklaus, "Direct leaching of rare earth elements and uranium from phosphate rocks," *Materials Science and Engineering*, vol. 479, pp. The 3rd International Conference on New Material and Chemical Industry 17–19 November 2018, Sanya, China, 2019. DOI:10.1088/1757-899X/479/1/012065

[20] F. Habashi, "Hydrometallurgy of phosphate rock and the recovery of uranium," *Uranium: Sources, Exposure and Environmental Effects*, Chapter 5, Nova Science Publishers, Inc., 2015. Available at: https://works.bepress.com/fathi_habashi/155/

[21] G. Xie, Q. Guan, F. Zhou, W. Yu, Z. Yin, H. Tang, Z. Zhang and R.A. Chi, "Critical review of the enhanced recovery of rare earth elements from phosphogypsum," *Molecules*, vol. 28, no. 17, pp.6284, 2023. DOI: https://doi.org/10.3390/molecules28176284

[22] H.K. Hapuhinna, R.D. Gunaratne, and H.M. Pitawala, "Development of a biomaterial from naturally occurring chloroapatite mineral for biomedical applications ", *International Scholarly and Scientific Research and Innovation,* vol. 12, no. 8, 2018. http://dr.lib.sjp.ac.lk/handle/123456789/9974

[23] S. Brahimi, A. Ressler, K. Boumchedda, M. Hamidouche, A. Kenzour, R. Djafar, M. Antunović, L. Bauer, P. Hvizdoš and H. Ivanković, "Preparation and characterization of biocomposites based on chitosan and biomimetic hydroxyapatite derived from natural phosphate rocks," *Materials Chemistry and Physics*, vol. 276, pp. 125421, 2022.DOI: https://doi.org/10.1016/j.matchemphys.2021.125421.

[24] R. Kareem, N. Bulut, and O. Kaygili, "Hydroxyapatite biomaterials: a comprehensive review of their properties, structures, medical applications, and fabrication methods," *Journal of Chemical Reviews*, vol. 6, no. 1, pp. 1-26, 2024. DOI: 10.48309/jcr.2024.415051.1253

[25] A. Patel, S. Namjoshi, S. Kumar, "Comparative experimental investigation of simple and V-shaped rib solar air heater," *International Journal of All Research Education and Scientific Methods*, vol. 11, no. 6, pp. 2993–2999, https://www.ijaresm.com/comparative-experimental-investigation-of-simple-and-v-shaped-rib-solar-air-heater

[26] M. J. Anderson, "Simple-comparative experiments done right," *Journal of Plastic Film and Sheeting*, vol. 40 no. 4, pp. 334–337, 2024. DOI: 10.1177/87560879241286598.

[27] G. Soto-Calle, A. Gómez-Zapata, N. Rojas-Reyes, and S. Díaz-Bello. "Production of hydroxyapatite from phosphoric rock", *DYNA*, vol. 91, no. 234, pp. 9-15, 2024. DOI: https://doi.org/10.15446/dyna.v91n234.113354

[28] B. Messai, I. Taieb, S. Ben Younes, B. Lartiges, E. Ben Salem and A. Ellafi. "Characterization of the Tunisian phosphate rock from Metlaoui-Gafsa basin and bio-leaching assays," *Sustainability*, vol. 15, pp. 7204, 2023. DOI: https://doi.org/10.3390/su15097204

[29] S. Nazarbekova, U. Nazarbek, P. Abdurazova and Y. Raiymbekov, "Study of solubility in the systems $CaO-P_2O_5-SO_3-H_2O$ and $CaO-P_2O_5-H_2O$ on the example of sulfuric-acid and phosphoric-acid decomposition of phosphoric slag. AIP Conference Proceedings, 2650, 020007, 2022. DOI: https://doi.org/10.1063/5.0107418

[30] H. Toama, A.W. Al-Ajeel and H. Waheeb, "Beneficiation of Akashat phosphate rocks by flotation process," *Engineering and Technology Journal*, vol. 33(A), no. 9, pp. 2255-2268, 2015. DOI:10.30684/etj.2015.116247

[31] A. Rasulov, S. Namazov and B. Sultonov, "Nitrogen-phosphate fertilizers based on activation of phosphorite powder with partially ammoniated mix of phosphoric and sulphuric acids," *Chemical Science International Journal*, vol. 29, no. 9, pp. 1-10, 2020. DOI:10.9734/CSJI/2020/v29i930201

[32] A. Chaabouni, C. Chtara, A. Nzihou, and H.E. Feki, "Study the nature and the effects of the impurities of phosphate rock in the plants of production of phosphoric acid," *Journal of Advances in Chemistry*, vol. 7, no. 2, pp. 1296–1299, 2008. DOI: https://doi.org/10.24297/jac.v7i2.5560

[33] P. Comodi, Y. Liu and M. Frezzotti, "Structural and vibrational behaviour of fluorapatite with pressure. Part II: in situ micro-Raman spectroscopic investigation," *Physics and Chemistry of Minerals*, vol. 28, pp. 225–231, 2001. DOI: https://doi.org/10.1007/s002690100155

[34] K. Litasov and N. Podgornykh, "Raman Spectroscopy of various phosphate minerals and occurrence of tuite in the Elga IIE iron meteorite," *Journal of Raman Spectroscopy*, 2017. DOI: 10.1002/jrs.5119.

[35] A. Antonakos, E. Liarokapis and T. Leventouri, "Micro Raman and FTIR studies of synthetic and natural apatites," *Biomaterials*, vol. 28, pp. 3043–3054, 2007. DOI: 10.1016/j.biomaterials.2007.02.028.

[36] H. Van Olphen and J. Fripiat, *Data Handbook for Clay Materials and Other Non-Metallic Minerals*. Pergamon Press, Oxford. 1979.

[37] B. Peng, X. Li, S. Xiang, L. Lei, M. Yang, L. Zhu and Y. Qi, "Release behavior of iodine during leaching and calcination of phosphate rock," *Environmental Science and Pollution Research*, vol. 28, pp. 31059–31070, 2021. DOI: https://doi.org/10.1007/s11356-021-12895-w

[38] K. Tõnsuaadu, K.A. Gross, L. Plūduma, and M. Veiderma, "A review on the thermal stability of calcium apatites," *Journal of Thermal Analysis and Calorimetry*, vol. 110, pp. 647–659, 2012. DOI: https://doi.org/10.1007/s10973-011-1877-y

[39] X.G. Li, Y. Lv, B.G. Ma, W.Q. Wang and S.W. Jian, "Decomposition kinetic characteristics of calcium carbonate containing organic acids by TGA," *Arabian Journal of Chemistry*, vol. 10, sp. 2, pp. S2534-S2538, 2017. DOI: https://doi.org/10.1016/j.arabjc.2013.09.026.

[40] V. Stanić, A. Radosavljević-Mihajlović, V. Živković-Radovanović, B. Nastasijević, M. Marinović-Cincović, J. Marković and M. Budimir, "Synthesis, structural characterisation and antibacterial activity of Ag+-doped fluorapatite nanomaterials prepared by neutralization method," *Applied Surface Science*, vol. 337, pp. 72–80, 2015. http://dx.doi.org/10.1016/j.apsusc.2015.02.065

[41] O. Suzuki, Y. Shiwaku, R. Hamai, "Octacalcium phosphate bone substitute materials: Comparison between properties of biomaterials and other calcium phosphate materials," *Dental Materials Journal*, vol. 39, no. 2, pp. 187-199, 2020. DOI: https://doi.org/10.4012/dmj.2020-001

[42] B. Ghiasi, Y. Sefidbakht, S, Mozaffari-Jovin, B. Gharehcheloo, M. Mehrarya, A. Khodadadi and V. Uskoković, "Hydroxyapatite as a biomaterial – a gift that keeps on giving," *Drug Development and Industrial Pharmacy*, vol. 46, no. 7, pp. 1035–1062. 2020. DOI: https://doi.org/10.1080/03639045.2020.1776321

[43] S. Mondal, S. Park, J. Choi, T. T. Ha-Vu, V. H. Minh-Doan, T. T. Vo, B. Lee, J. Oh, "Hydroxyapatite: A journey from biomaterials to advanced functional materials," *Advances in colloid and interface science*, vol. 321, pp. 103013, 2023. DOI: https://doi.org/10.1016/j.cis.2023.103013

[44] Z. Wang, Q. Li., S. Ren, H. Zhang, J. Chen, A. Li, and Y. Chen, "Composite monetite/amorphous calcium phosphate bone cement promotes bone regeneration". *Ceramics International*, 49(5), 7888–7904. 2024 DOI: https://doi.org/10.1016/j.ceramint.2022.10.296

[45] H. Yuan, and K. de Groot, "Calcium phosphate biomaterials: an overview," Learning from Nature How to Design New Implantable Biomaterialsis: From Biomineralization Fundamentals to Biomimetic Materials and Processing Routes. NATO Science Series II: Mathematics, Physics and Chemistry, vol 171. Springer, Dordrecht. 2004.DOI: https://doi.org/10.1007/1-4020-2648-X_3

[46] L. Chow, "Next generation calcium phosphate-based biomaterials," *Dental Materials Journal*, vol. 28, no. 1, pp. 1-10, 2009. DOI: 10.4012/dmj.28.1

[47] J. Jeong, J.H. Kim, J.H. Shim, N.S. Hwang and C.Y. Heo, "Bioactive calcium phosphate materials and applications in bone regeneration," *Biomaterials Research*, vol. 23, no. 4, 2019. https://doi.org/10.1186/s40824-018-0149-3

[48] X. Hou, L. Zhang, Z. Zhou, X. Luo, T. Wang, X. Zhao, B. Lu, F. Chen and L. Zheng, "Calcium phosphate-based biomaterials for bone repair," *Journal of Functional Biomaterials*, vol. 13, no. 4, pp. 187, 2022. DOI: 10.3390/jfb13040187.